Supporting Information:

Simulating electronic structure on bosonic

quantum computers

Rishab Dutta,[†] Nam P. Vu,[†,‡,¶] Chuzhi Xu,[†] Delmar G. A. Cabral,[†] Ningyi Lyu,[†] Alexander V. Soudackov,[†] Xiaohan Dan,[†] Haote Li,[†] Chen Wang,[§] and Victor S. Batista[†,∥]

†Department of Chemistry, Yale University, New Haven, CT, USA 06520

‡Department of Chemistry, Lafayette College, Easton, PA, USA 18042

¶Department of Electrical and Computer Engineering, Lafayette College, Easton, PA, USA 18042

§Department of Physics, University of Massachusetts-Amherst, Amherst, MA, USA 01003

∥Yale Quantum Institute, Yale University, New Haven, CT, USA 06511

Overview of the electronic structure problem

Here, we provide further context and motivation for the electronic structure problem. The molecular Hamiltonian in atomic units can be written as[S1]

$$\mathcal{H} = -\frac{1}{2} \sum_i \nabla_i^2 - \frac{1}{2} \sum_A \frac{\nabla_A^2}{M_A} - \sum_i \sum_A \frac{Z_A}{r_{iA}} + \sum_i \sum_{j>i} \frac{1}{r_{ij}} + \sum_A \sum_{B>A} \frac{Z_A Z_B}{R_{AB}}, \quad (1)$$

where i, j are electron indices, A, B are nuclear indices, ∇_i^2 and ∇_A^2 are Laplacian operators representing differentiation with respect to the coordinates of the ith electron and A^{th} nucleus,

M_A and Z_A are the mass and atomic number of nucleus A, $r_{iA} = |\mathbf{r}_i - \mathbf{R}_A|$ is the distance between i^{th} electron and A^{th} nucleus, $r_{ij} = |\mathbf{r}_i - \mathbf{r}_j|$ is the distance between i^{th} and j^{th} electrons, and $R_{AB} = |\mathbf{R}_A - \mathbf{R}_B|$ is the distance between A^{th} and B^{th} nuclei. The operator terms in Eq. (1) represent the kinetic energy of electrons, kinetic energy of nuclei, Coulombic attraction between electrons and nuclei, repulsion between electrons, and repulsion between nuclei, respectively.

The Born–Oppenheimer approximation assumes the molecular electrons are moving in the field of fixed nuclei since they are much lighter.[S1] This allows one to neglect the nuclear kinetic energy term in Eq. (1) and consider the nuclear-nuclear repulsion term to be constant. Thus, the remaining terms of Eq. (1) constitute the molecular electronic structure Hamiltonian

$$\mathcal{H}_{\text{elec}} = -\frac{1}{2} \sum_i \nabla_i^2 - \sum_i \sum_A \frac{Z_A}{r_{iA}} + \sum_i \sum_{j>i} \frac{1}{r_{ij}}. \tag{2}$$

Our goal is to solve the time-independent Schrödinger equation for the molecular electronic structure

$$\mathcal{H}_{\text{elec}} \Psi_\mu(\mathbf{r}) = E_\mu \Psi_\mu(\mathbf{r}) \tag{3}$$

where $\{\Psi_\mu\}$ are the electronic wavefunctions with corresponding energies $\{E_\mu\}$ for a given molecular nuclear coordinates with $\{\mathbf{r}_j\}$ being the set of electronic coordinates. As an example, Ψ_0 and E_0 are the ground electronic wavefunction and its energy. Finding the $\{\Psi_n\}$ wavefunctions on a classical computer is a notoriously hard problem because of the combinatorial growth of the dimensionality with increasing number of electrons N in the molecule. This is where quantum computing promises to be impactful.

An electronic wavefunction $\Psi(\mathbf{r})$ depends on a set of N electron coordinates $\{\mathbf{r}_j\}$. However, one should also include the electron spin into the picture, and denote the wavefunction as $\Psi(\mathbf{x})$ instead, where $\mathbf{x}$ represents the combined spatial and spin coordinates of the electrons. Spin does not fundamentally arise in the non-relativistic premise of electronic structure theory. Nevertheless, spin must be included as a bookkeeping tool to respect the fermionic

antisymmetry of electrons

$$\Psi(\cdots,\mathbf{x}_j,\cdots,\mathbf{x}_k,\cdots) = -\Psi(\cdots,\mathbf{x}_k,\cdots,\mathbf{x}_j,\cdots), \tag{4}$$

even in approximate wavefunctions. A good starting point for approximately solving the electronic structure is the Hartree–Fock (HF) method,[S1] which transform the many-electron problem of Eq. (3) to an effective one-electron problem in the mean-field created by the other electrons. The HF method provides M number ($M > N$) of orthonormal one-electron functions $\{\chi_p(\mathbf{x})\}$, called the molecular spin-orbitals. We are assuming M to be an even integer since there is an underlying $M/2$ number of spatial functions $\{\phi_p(\mathbf{r})\}$ which can associate with either up-spin $\alpha(\omega)$ or down-spin $\beta(\omega)$ functions

$$\chi_{2p\uparrow}(\mathbf{x}) \equiv \phi_p(\mathbf{r})\,\alpha(\omega), \quad \chi_{2p\downarrow} \equiv \phi_p(\mathbf{x})\,\beta(\omega). \tag{5}$$

Thus, N electrons in M molecular spin-orbitals give rise to $\binom{M}{N}$ number of many-electron basis states, each of which is an antisymmetrized product state

$$|p_1,\cdots,p_N\rangle_F \equiv \frac{1}{\sqrt{N!}}
\begin{vmatrix}
\chi_{p_1}(\mathbf{x}_1) & \cdots & \chi_{p_N}(\mathbf{x}_1) \\
\chi_{p_1}(\mathbf{x}_2) & \cdots & \chi_{p_N}(\mathbf{x}_2) \\
\cdots & \ddots & \cdots \\
\chi_{p_1}(\mathbf{x}_N) & \cdots & \chi_{p_N}(\mathbf{x}_N)
\end{vmatrix}, \tag{6}$$

where $0 \le p_1 < \cdots < p_N \le M - 1$. The wavefunction in Eq. (6) is the so-called Slater determinant and based on the ordering of $\{p_j\}$ indices, approximates the exact ground and excited electronic states. For example, the Slater determinant $|0,\cdots,N-1\rangle_F$ is the electronic ground state wavefunction under the HF approximation.

Justification of the state mapping

The state mapping described in the Main Text is justified if we can prove that acting with bosonic operators $\{b_j^\dagger, b_j\}$ on the mapped fermionic states still preserve their commutation relations. We follow the derivation done in Ref. S2 here, although a similar justification was first given by Ref. S3.

The first step to deduce the action of bosonic creation operators on a Slater determinant is to apply the state mapping to get

$$b_j^\dagger \left|p_1, \cdots, p_N\right\rangle_F = b_j^\dagger \left|q_1, \cdots, q_N\right\rangle_B = \sqrt{q_j + 1} \left|q_1, \cdots, q_j + 1, \cdots, q_N\right\rangle_B, \tag{7}$$

which can be again mapped back to

$$b_j^\dagger \left|p_1, \cdots, p_N\right\rangle_F = \sqrt{p_{N-j+1} - p_{N-j}} \left|p_1, \cdots, p_{N-k}, p_{N-k+1} + 1, \cdots, p_N + 1\right\rangle_F, \tag{8}$$

where $j < N$. The same expression for the special case of $j = N$ is given by

$$b_N^\dagger \left|p_1, \cdots, p_N\right\rangle_F = \sqrt{p_1 + 1} \left|p_1 + 1, \cdots, p_N + 1\right\rangle_F, \tag{9}$$

The action of bosonic annihilation operators on a Slater determinant can be similarly derived as

$$b_j \left|p_1, \cdots, p_N\right\rangle_F = \sqrt{p_{N-j+1} - p_{N-j} - 1} \left|p_1, \cdots, p_{N-k}, p_{N-k+1} - 1, \cdots, p_N - 1\right\rangle_F, \tag{10}$$

when $j < N$ and

$$b_N \left|p_1, \cdots, p_N\right\rangle_F = \sqrt{p_1} \left|p_1 - 1, \cdots, p_N - 1\right\rangle_F. \tag{11}$$

Let us now combine Eq. (8) and Eq. (10) to arrive at

$$b_j b_k^\dagger \left| p_1, \cdots, p_N \right\rangle_F = \sqrt{(p_{N-k+1} - p_{N-k})(p_{N-j+1} - p_{N-j} - 1)}$$

$$\times \left| p_1, \cdots, p_{N-k}, p_{N-k+1} + 1, \cdots, p_{N-j} + 1, p_{N-j+1}, \cdots, p_N \right\rangle_F, \qquad (12)$$

where $j < k$. Similarly, by reversing the order of the bosonic operators, we get

$$b_k^\dagger b_j \left| p_1, \cdots, p_N \right\rangle_F = \sqrt{(p_{N-k+1} - p_{N-k})(p_{N-j+1} - p_{N-j} - 1)}$$

$$\times \left| p_1, \cdots, p_{N-k}, p_{N-k+1} + 1, \cdots, p_{N-j} + 1, p_{N-j+1}, \cdots, p_N \right\rangle_F, \qquad (13)$$

where $j < k$. Thus, the right hand sides of Eq. (12) and Eq. (13) are the same, which proves $[b_j, b_k^\dagger] = 0$ for $j < k$. The $j > k$ case can be similarly derived as above. Let us now consider the $j = k$ case

$$b_k b_k^\dagger \left| p_1, \cdots, p_N \right\rangle_F = (p_{N-k+1} - p_{N-k}) \left| p_1, \cdots, p_N \right\rangle_F. \qquad (14)$$

Similarly, by reversing the order, we get

$$b_k^\dagger b_k \left| p_1, \cdots, p_N \right\rangle_F = (p_{N-k+1} - p_{N-k} - 1) \left| p_1, \cdots, p_N \right\rangle_F. \qquad (15)$$

Thus, Eq. (14) and Eq. (15) shows that $[b_k, b_k^\dagger] = 1$, which proves that the state mapping preserves the relation $[b_j, b_k^\dagger] = \delta_{jk}$.

Derivation of the operator mapping

The derivation of the mapping $\{E_q^p\}$ operators is shown in Ref. S2, which we call Dhar–Mandal–Suryanarayana (DMS) mapping or simply direct mapping. We gain insight into the derivation here by discussing all the steps for the specific cases of $N = 1$ and $N = 2$.

Let us first discuss the operator mapping with an $N = 1$ system. The state mapping is

then simply $|j\rangle_F \leftrightarrow |j\rangle_B$, where the one-particle states are defined as

$$|j\rangle_F \equiv f_j^\dagger |-\rangle_F , \quad |j\rangle_B \equiv \frac{b_j^\dagger}{\sqrt{j!}} |0\rangle_B . \tag{16}$$

Let us figure out how the bilinear fermionic operators act on the state $|j\rangle_B$ by using the state mapping. The states $\{|j\rangle_F\}$ are eigenstate of the number operator E_p^p, and combining this with the state mapping leads to

$$E_p^p |j\rangle_F = \delta_{pj} |j\rangle_B = (|j\rangle \langle p|) |j\rangle_B = (|p\rangle \langle p|) |j\rangle_B , \tag{17}$$

where $|p\rangle \langle p|$ is the projection operator in the bosonic Fock basis with the subscripts "B" suppressed to avoid symbolic clutter. Since $|j\rangle_B$ can now be mapped back to $|j\rangle_F$, the number operator is thus mapped as

$$E_p^p \mapsto |p\rangle \langle p| , \tag{18}$$

$p = 0, 1, \cdots, M - 1$. Similarly, acting with the off-diagonal bilinear fermionic operator on $|j\rangle_F$ leads to

$$E_{q+p}^q |j\rangle_F = \delta_{qj} f_{j+p}^\dagger |-\rangle_F = \delta_{qj} |j + p\rangle_F , \tag{19}$$

which maps to the state $|j + p\rangle_B$. We can now write

$$E_q^{q+p} |j\rangle_F = (\sigma^\dagger)^p \delta_{q,j} |j\rangle_B = (\sigma^\dagger)^p (|q\rangle \langle q|) |j\rangle_B . \tag{20}$$

Since $|j\rangle_B$ can now be mapped back to $|j\rangle_F$, the E_q^{q+p} operator can be mapped as

$$E_q^{q+p} \mapsto (\sigma^\dagger)^p |q\rangle \langle q| , \tag{21}$$

where $q = 1, \cdots, M-1$ and $p = 1, \cdots, M-p-1$. Because of its adjoint relation $(E_q^p)^\dagger = E_p^q$,

mapping bilinear fermionic operators $\{E_q^p\}$ for $p \geq q$ is sufficient.

Let us now discuss the $N = 2$ case, for which the state mapping is given by, $|p, q\rangle_F \leftrightarrow |j, k\rangle_B$. Let us start our derivation by writing down how the number operator E_r^r acts on an arbitrary Slater determinant

$$E_r^r |p, q\rangle_F = (\delta_{p,r} + \delta_{q,r}) |p, q\rangle_F, \tag{22}$$

and after applying the state mapping back and forth, we arrive at

$$\begin{aligned}
E_r^r |p, q\rangle_F &\mapsto (\delta_{k,r} + \delta_{j+k,r-1}) |j, k\rangle_B \\
&= \left[\delta_{k,r} + \sum_{a+b=r-1} \delta_{j,a}\, \delta_{k,b} \right] |j, k\rangle_B \\
&= \left[\mathbb{I} \otimes |r\rangle \langle r| + \sum_{a+b=r-1} |a, b\rangle \langle a, b| \right] |j, k\rangle_B \\
&\mapsto \left[\mathbb{I} \otimes |r\rangle \langle r| + \sum_{a+b=r-1} |a, b\rangle \langle a, b| \right] |p, q\rangle_F, \tag{23}
\end{aligned}$$

where $\mathbb{I}$ is the identity operator acting on the first mode. We extended the projection operator trick in the derivation of the $N = 1$ system here, i.e., the goal is to find a Kronecker delta involving one of the indices (j and k) corresponding to the two modes. We can now redefine the dummy indices above and express the mapping for the number operators as

$$E_p^p \mapsto \mathbb{I} \otimes |p\rangle \langle p| + \sum_{a+b=p-1} |a, b\rangle \langle a, b|. \tag{24}$$

Let us now map the off-diagonal operators. We first act E_s^{s+r} on an arbitrary Slater determinant

$$E_s^{s+r} |p, q\rangle_F = \delta_{p,s}\, f_{p+r}^\dagger f_q^\dagger |-\rangle_F + \delta_{q,s}\, f_p^\dagger f_{q+r}^\dagger |-\rangle_F, \tag{25}$$

which can be further written as

$$E_s^{s+r} \left| p, q \right\rangle_F = \delta_{p,s} \left(\sum_{a=p+1}^{q-1} \delta_{p+r,a} \left| p+r, q \right\rangle_F - \sum_{a=q+1}^{\infty} \delta_{p+r,a} \left| q, p+r \right\rangle_F \right)$$
$$+ \delta_{q,s} \left| p, q+r \right\rangle_F . \tag{26}$$

Similar to the derivation for the $N = 1$ case, we now apply the state mapping and the normalized bosonic operators. The third term of Eq. (26) then reduces to

$$\delta_{q,s} \left| p, q+r \right\rangle_F \mapsto \delta_{j+k,s-1} \left| j+r, k \right\rangle_B = (\sigma_1^\dagger)^r \, \delta_{j+k,s-1} \left| j, k \right\rangle_B , \tag{27}$$

Similarly the first term of Eq. (26) can be rewritten as

$$\delta_{p,s} \sum_{a=p+1}^{q-1} \delta_{p+r,a} \left| p+r, q \right\rangle_F \mapsto \delta_{p,s} \sum_{a=p+1}^{q-1} \delta_{p+r,a} \left| j-r, k+r \right\rangle_B$$
$$= \sigma_1^r \, (\sigma_2^\dagger)^r \sum_{a=0}^{\infty} \delta_{j,r+a} \, \delta_{k,s} \left| j, k \right\rangle_B , \tag{28}$$

whereas the second term of Eq. (26) turns to

$$\delta_{p,s} \sum_{a=q+1}^{\infty} \delta_{p+r,a} \left| q, p+r \right\rangle_F \mapsto \delta_{p,s} \sum_{a=0}^{\infty} \delta_{p+r,a+q+1} \left| r-2-j, j+k+1 \right\rangle_B$$
$$= \sum_{a=0}^{r-2} (\sigma_1^\dagger)^{r-2-a} \, \sigma_1^a \, (\sigma_2^\dagger)^{a+1} \, \delta_{j,a} \, \delta_{k,s} \left| j, k \right\rangle_B . \tag{29}$$

Applying the projection operator relation and the state mapping back to the Slater determinants, the action of the E_s^{s+r} on an arbitrary Slater determinant can now be written

as

$$E_s^{s+r} \ket{p,q}_F = \left[\sigma_1^r (\sigma_2^\dagger)^r \sum_{a=0}^{\infty} \ket{r+a,s} \bra{r+a,s} - \sum_{a=0}^{r-2} (\sigma_1^\dagger)^{r-2-a} \sigma_1^a (\sigma_2^\dagger)^{a+1} \ket{a,s} \bra{a,s} \right.$$
$$\left. + (\sigma_1^\dagger)^r \sum_{a+b=s-1} \ket{a,b} \bra{a,b} \right] \ket{p,q}_F. \tag{30}$$

We can now redefine the dummy indices above and express the mapping for the off-diagonal operators as

$$E_q^{q+p} \mapsto \sigma_1^p (\sigma_2^\dagger)^p \sum_{a=0}^{\infty} \ket{p+a,q} \bra{p+a,q} - \sum_{a=0}^{p-2} (\sigma_1^\dagger)^{p-2-a} \sigma_1^a (\sigma_2^\dagger)^{a+1} \ket{a,q} \bra{a,q}$$
$$+ (\sigma_1^\dagger)^p \sum_{a+b=q-1} \ket{a,b} \bra{a,b}. \tag{31}$$

Thus, we have shown how to derive the DMS operator mapping for the $N=1$ and $N=2$ cases.

General DMS mapping expression

The expression for the DMS mapping of $\{E_q^p\}$ with $p > q$ is given by[S2]

$$
\begin{aligned}
E_q^{q+p} \mapsto &\sum_{\substack{r_1+\cdots+r_N \\ = q-N+1}} (\sigma_1^\dagger)^p \, \mathcal{P}_{r_1,\cdots,r_N} + \sum_{a=0}^\infty \sum_{\substack{r_2+\cdots+r_N \\ = q-N+2}} \sigma_1^p (\sigma_2^\dagger)^p \, \mathcal{P}_{p+a,r_2,\cdots,r_N} \\
&- \sum_{\mu=0}^{p-2} \sum_{\substack{r_2+\cdots+r_N \\ = q-N+2}} (\sigma_1^\dagger)^{p-2-\mu} \sigma_1^\mu (\sigma_2^\dagger)^{\mu+1} \, \mathcal{P}_{\mu,r_2,\cdots,r_N} \\
&+ \sum_{k=2}^{N-1} \Bigg[\mathcal{I}_{k-1} \otimes \sum_{a=0}^\infty \sum_{\substack{r_{k+1}+\cdots+r_N \\ = q-N+k+1}} \sigma_k^p (\sigma_{k+1}^\dagger)^p \, \mathcal{P}_{p+a,r_{k+1},\cdots,r_N} \\
&- \mathcal{I}_{k-2} \otimes \sum_{a=0}^\infty \sum_{\mu=0}^{p-2} \sum_{r_{k-1}=a+1}^{p+a-1} \sum_{\substack{r_{k+1}+\cdots+r_N \\ = q-N+k+1}} \mathcal{T}_{p,k,\mu}^1 \, \mathcal{P}_{r_{k-1},\mu,r_{k+1},\cdots,r_N} \\
&+ (-1)^k \Bigg(\sum_{r_1=0}^\infty \cdots \sum_{r_k=0}^\infty - \sum_{a=0}^\infty \sum_{\substack{r_1+\cdots+r_k \\ = p+a-k}} \Bigg) \sum_{\substack{r_{k+1}+\cdots+r_N \\ = q-N+k+1}} \mathcal{T}_{p,k,\mu_1,\cdots,\mu_k}^2 \, \mathcal{P}_{r_1,\cdots,r_N} \\
&+ \sum_{j=2}^{k-1} (-1)^j \, \mathcal{I}_{k-j-1} \otimes \sum_{a=0}^\infty \Bigg(\sum_{\substack{r_{k-j}+\cdots+r_k \\ = p+a-j}} \sum_{\substack{r_{k+1}+\cdots+r_N \\ = q-N+k+1}} \mathcal{T}_{p,k,j,r_{k-j+1},\cdots,r_k}^3 \, \mathcal{P}_{r_{k-j},\cdots,r_N} \\
&- \sum_{\substack{r_{k-j+1}+\cdots+r_k \\ = p+a-j}} \sum_{\substack{r_{k+1}+\cdots+r_N \\ = q-N+k+1}} \mathcal{T}_{p,k,j,r_{k-j+1},\cdots,r_k}^3 \, |0\rangle \langle 0| \otimes \mathcal{P}_{r_{k-j+1},\cdots,r_N} \Bigg) \Bigg],
\end{aligned}
\tag{32}
$$

where $q = 0, \cdots, M-2$ and $p = 1, \cdots, M-q-1$ and the operators $\{\mathcal{T}^\mu\}$ are defined in Table S1. All the summations in Eq. (32) will naturally truncate following the highest Fock state allowed for a qumode based on the state mapping described in the Main Text . There are $\mathcal{O}(N^2)$ number of terms in Eq. (32) that need to be taken care of in case of computing the expectation value of the operator E_q^{q+p}. The expression for $\{E_q^p\}$ with $p < q$ can be found by taking the Hermitian conjugate of Eq. (32), while the mapping for $p = q$ is given in the Main Text .

Table S1: Definitions for the intermediate operator terms used in Eq. (32).

Operator	Definition
$\mathcal{T}^1_{p,k,\mu}$	$\sigma_{k-1}^{p-1-\mu}\,(\sigma_k^\dagger)^{p-2-\mu}\,\sigma_k^\mu\,(\sigma_{k+1}^\dagger)^{\mu+1}$
$\mathcal{T}^2_{p,k,r_1,\cdots,r_k}$	$(\sigma_1^\dagger)^{p-1-k-(r_1+\cdots+r_k)}\,\sigma_1^{r_1}\,(\sigma_2^\dagger)^{r_1}\,\cdots\sigma_{k-1}^{r_{k-1}}\,(\sigma_k^\dagger)^{r_{k-1}}\,\sigma_k^{r_k}\,(\sigma_{k+1}^\dagger)^{r_k+1}$
$\mathcal{T}^3_{p,k,j,\mu_{k-j+1},\cdots,\mu_k}$	$\sigma_{k-j}^{p-j-(\mu_{k-j+1}+\cdots+\mu_k)}\,(\sigma_{k-j+1}^\dagger)^{p-j-1-(\mu_{k-j+1}+\cdots+\mu_k)}$ $\times\,\sigma_{k-j+1}^{\mu_{k-j+1}}\,(\sigma_{k-j+2}^\dagger)^{\mu_{k-j+1}}\,\cdots\,\sigma_{k-1}^{\mu_{k-1}}\,(\sigma_k^\dagger)^{\mu_{k-1}}\,\sigma_k^{\mu_k}\,(\sigma_{k+1}^\dagger)^{\mu_k+1}$

Bosonic Hamiltonian for the dihydrogen molecule

The Hamiltonian of the dihydrogen molecule in a minimal basis can be written as[S4]

$$H_F = h_0^0\,f_0^\dagger f_0 + h_1^1\,f_1^\dagger f_1 + h_2^2\,f_2^\dagger f_2 + h_3^3\,f_3^\dagger f_3 + v_{10}^{01}\,f_0^\dagger f_1^\dagger f_1 f_0 + v_{32}^{23}\,f_2^\dagger f_3^\dagger f_3 f_2$$

$$+\, v_{30}^{03}\,f_0^\dagger f_3^\dagger f_3 f_0 + v_{21}^{12}\,f_1^\dagger f_2^\dagger f_2 f_1 + (v_{20}^{02} - v_{02}^{02})\,f_0^\dagger f_2^\dagger f_2 f_0 + (v_{31}^{13} - v_{13}^{13})\,f_1^\dagger f_3^\dagger f_3 f_1$$

$$+\, v_{12}^{03}\,(f_0^\dagger f_3^\dagger f_1 f_2 + \text{h.c.}) + v_{32}^{01}\,(f_0^\dagger f_1^\dagger f_3 f_2 + \text{h.c.}), \tag{33}$$

which can be written in terms of the bilinear fermionic operators

$$H_F = (h_0^0 + v_{10}^{01} + v_{30}^{03} + v_{20}^{02} - v_{02}^{02})\,E_0^0 + (h_1^1 + v_{21}^{12} + v_{31}^{13} - v_{13}^{13})\,E_1^1 + (h_2^2 + v_{32}^{23})\,E_2^2 + h_3^3\,E_3^3$$

$$-\, v_{10}^{01}\,E_1^0 E_0^1 - v_{32}^{23}\,E_3^2 E_2^3 - v_{30}^{03}\,E_3^0 E_0^3 - v_{21}^{12}\,E_2^1 E_1^2 - (v_{20}^{02} - v_{02}^{02})\,E_2^0 E_0^2 - (v_{31}^{13} - v_{13}^{13})\,E_3^1 E_1^3$$

$$-\, v_{12}^{03}\,(E_1^0 E_2^3 + \text{h.c.}) - v_{32}^{01}\,(E_3^0 E_2^1 + \text{h.c.}), \tag{34}$$

which means that we need to map the lone operators E_p^p with $p = 0, 1, 2, 3$, the *symmetric* operator couples $E_q^p E_p^q$ with $p = 0, 1, 2$ and $q = p + 1$, and the *transition* operator couples $E_1^0 E_2^3$ and $E_3^0 E_2^1$.

Let us map each of the operator terms of the Hamiltonian in Eq. (34). The maps

corresponding to the operator terms with single bilinear fermionic operators are

$$E_0^0 \mapsto \mathbb{I} \otimes |0\rangle \langle 0| , \tag{35a}$$

$$E_1^1 \mapsto \mathbb{I} \otimes |1\rangle \langle 1| + |0,0\rangle \langle 0,0| , \tag{35b}$$

$$E_2^2 \mapsto \mathbb{I} \otimes |2\rangle \langle 2| + |0,1\rangle \langle 0,1| + |1,0\rangle \langle 1,0| , \tag{35c}$$

$$E_3^3 \mapsto |0,2\rangle \langle 0,2| + |1,1\rangle \langle 1,1| + |2,0\rangle \langle 2,0| , \tag{35d}$$

where we have truncated the mapping expression based on the relevant bosonic subspace for our problem. The expressions after mapping the symmetric operator terms are

$$E_1^0 E_0^1 \mapsto |1,0\rangle \langle 1,0| + |2,0\rangle \langle 2,0| , \tag{36a}$$

$$E_3^0 E_0^3 \mapsto |0,0\rangle \langle 0,0| + |1,0\rangle \langle 1,0| , \tag{36b}$$

$$E_2^1 E_1^2 \mapsto |0,0\rangle \langle 0,0| + |1,1\rangle \langle 1,1| + |2,1\rangle \langle 2,1| , \tag{36c}$$

$$E_2^0 E_0^2 \mapsto |0,0\rangle \langle 0,0| + |2,0\rangle \langle 2,0| , \tag{36d}$$

$$E_3^1 E_1^3 \mapsto |0,0\rangle \langle 0,0| + |0,1\rangle \langle 0,1| + |2,1\rangle \langle 2,1| , \tag{36e}$$

$$E_3^2 E_2^3 \mapsto |0,1\rangle \langle 0,1| + |1,0\rangle \langle 1,0| + |1,2\rangle \langle 1,2| + |2,2\rangle \langle 2,2| . \tag{36f}$$

The rest of the operator terms are similarly mapped as

$$E_1^0 E_2^3 \mapsto |2,0\rangle \langle 0,1| , \tag{37a}$$

$$E_3^0 E_2^1 \mapsto -|0,0\rangle \langle 0,2| . \tag{37b}$$

We now combine Eq. (35), Eq. (36), and Eq. (37) to arrive at

$$H_B = \left(h_0^0 + h_1^1 + v_{10}^{01} \right) |0,0\rangle \langle 0,0| + \left(h_1^1 + h_2^2 + v_{21}^{12} \right) |0,1\rangle \langle 0,1|$$
$$+ \left(h_0^0 + h_2^2 + v_{20}^{02} - v_{02}^{02} \right) |1,0\rangle \langle 1,0| + \left(h_1^1 + h_3^3 + v_{31}^{13} - v_{13}^{13} \right) |1,1\rangle \langle 1,1|$$
$$+ \left(h_2^2 + h_3^3 + v_{32}^{23} \right) |0,2\rangle \langle 0,2| + \left(h_0^0 + h_3^3 + v_{30}^{03} \right) |2,0\rangle \langle 2,0|$$
$$+ v_{32}^{01} \left(|0,0\rangle \langle 0,2| + \text{h.c.} \right) - v_{12}^{03} \left(|2,0\rangle \langle 0,1| + \text{h.c.} \right). \tag{38}$$

We can simplify even more by taking advantage of the symmetries of the four spin-orbitals of the H_2 molecule in a minimal basis, which leads to the following relations[S4]

$$h_0^0 = h_1^1, \tag{39a}$$

$$h_2^2 = h_3^3, \tag{39b}$$

$$v_{20}^{02} = v_{31}^{13} = v_{21}^{12} = v_{30}^{03}, \tag{39c}$$

$$v_{02}^{02} = v_{12}^{03} = v_{32}^{01} = v_{13}^{13}. \tag{39d}$$

Thus, we can finally map the Hamiltonian in Eq. (34) to the bosonic form below

$$H_B = \left(h_0^0 + h_1^1 + v_{10}^{01} \right) |0,0\rangle \langle 0,0| + \left(h_0^0 + h_2^2 + v_{20}^{02} \right) |0,1\rangle \langle 0,1|$$
$$+ \left(h_0^0 + h_2^2 + v_{20}^{02} - v_{02}^{02} \right) |1,0\rangle \langle 1,0| + \left(h_0^0 + h_2^2 + v_{20}^{02} - v_{02}^{02} \right) |1,1\rangle \langle 1,1|$$
$$+ \left(2h_2^2 + v_{32}^{23} \right) |0,2\rangle \langle 0,2| + \left(h_0^0 + h_2^2 + v_{20}^{02} \right) |2,0\rangle \langle 2,0|$$
$$+ v_{02}^{02} \left(|0,0\rangle \langle 0,2| + \text{h.c.} \right) - v_{02}^{02} \left(|2,0\rangle \langle 0,1| + \text{h.c.} \right). \tag{40}$$

The final form of the Hamiltonian mapping of Eq. (34) becomes

$$H_F \mapsto H_B = g_1 |0,0\rangle \langle 0,0| + g_2 |0,2\rangle \langle 0,2| + g_3 \big(|0,1\rangle \langle 0,1| + |2,0\rangle \langle 2,0| \big)$$
$$+ g_4 \big(|1,0\rangle \langle 1,0| + |1,1\rangle \langle 1,1| \big) + g_5 \big(|0,0\rangle \langle 0,2| + \text{h.c.} \big)$$
$$- g_5 \big(|2,0\rangle \langle 0,1| + \text{h.c.} \big), \tag{41}$$

where the scalars $\{g_p\}$ are defined in Table S2.

Table S2: The bosonic Hamiltonian coefficients of the dihydrogen molecule in a minimal basis defined in Eq. (41) in terms of the one-electron and two-electron integrals.

Coefficient	Definition
g_1	$h_0^0 + h_1^1 + v_{10}^{01}$
g_2	$2h_2^2 + v_{32}^{23}$
g_3	$h_0^0 + h_2^2 + v_{20}^{02}$
g_4	$h_0^0 + h_2^2 + v_{20}^{02} - v_{02}^{02}$
g_5	v_{02}^{02}

The dependence of the bosonic Hamiltonian coefficients of Eq. (41) on the H–H bond distance is shown in Figure S1. The simplification of the bosonic Hamiltonian originates from the fact that the projection operators should not correspond to a basis state that is outside of the physical Hilbert space for the dihydrogen molecule. Thus, the bosonic Hamiltonian in Eq. (41) can also be understood as a Hamiltonian of two qutrits, i.e., qudits with three dimensions. The mapped bosonic Hamiltonian has six physical Fock basis states and the corresponding matrix heatmap is shown in Figure S2 for the H–H bond distance of 0.7414 Å, which matches exactly with its corresponding fermionic FCI matrix elements.

Let us now discuss the expectation values of the Hamiltonian in Eq. (41) given a bosonic state. There are two classes of operator terms possible for a bosonic Hamiltonian expressed in terms of tensor products of projection operators, namely, the photon counting operator such as $|1,0\rangle \langle 1,0|$ and photon transfer operators such as $|2,0\rangle \langle 0,1| + \text{h.c.}$. The expectation values for the photon counting operators are easy to interpret. For example, the expectation
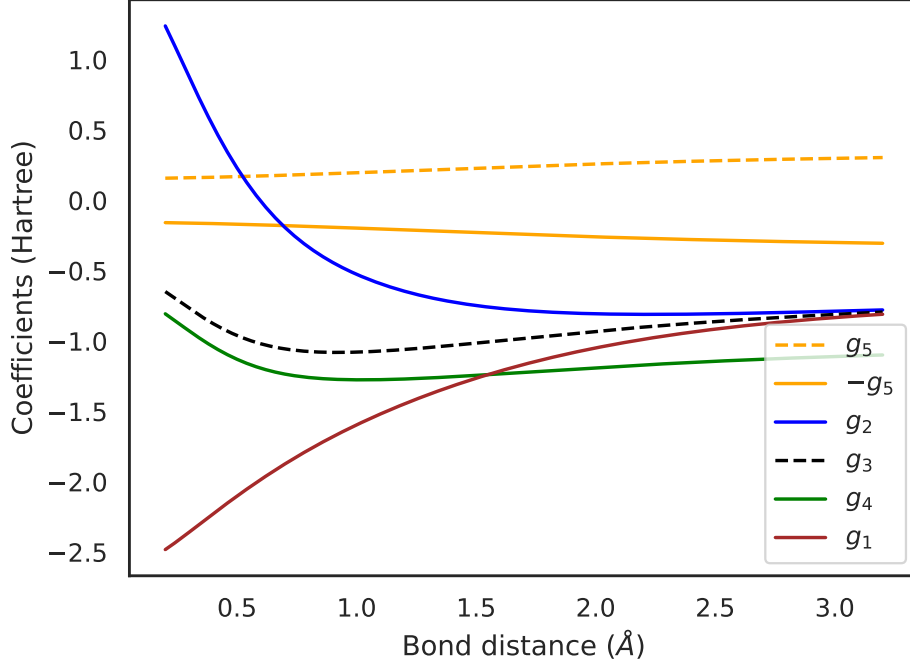
Figure S1: The parametric dependence of the mapped bosonic Hamiltonian coefficients for the dihydrogen molecule in the STO-3G minimal basis, as defined in Eq. (41), on the H–H bond distance. The Hamiltonian coefficients are defined in Table S2.

value of $|1,0\rangle\langle 1,0|$ for a given trial state

$$\langle\psi|(|1,0\rangle\langle 1,0|)|\psi\rangle = |\langle 1,0|\psi\rangle|^2 \tag{42}$$

is equivalent to the probability of measuring one photon in the first and zero photons in the second qumode. The photon counting can be measured by optical detectors in the case of photonic quantum computing,[S5,S6] or using cavity-transmon parity measurements in the case of cQED approach.[S7]

Computing the expectation value of photon transfer operators can be done via at least two ways. A conceptually straightforward approach involves generalization of the qubit-based Pauli-X operator expectation value for a pairs of qudit states. Let us elaborate with a specific example below

$$\bar{X} \equiv |2,0\rangle\langle 0,1| + \text{h.c.} = \bar{H}\bar{Z}\bar{H}, \tag{43}$$
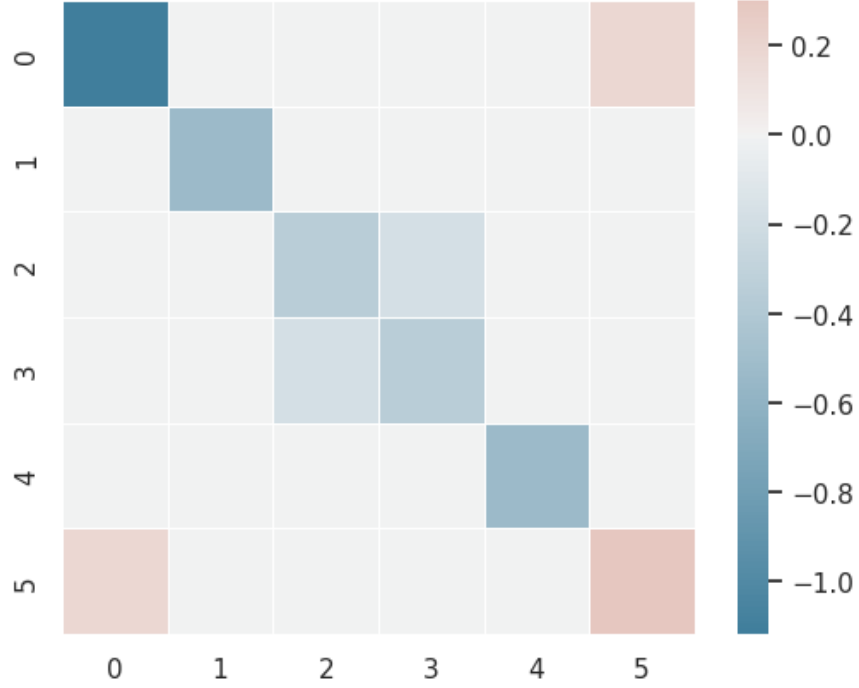
Figure S2: Heatmap of the Hamiltonian matrix elements for the dihydrogen molecule in the STO-3G minimal basis after the direct mapping. The matrix elements are computed for the fixed H–H bond distance of 0.7414 Å and match exactly with their analogous fermionic Hamiltonian matrix elements.

where the generalizations of Pauli-Z and Hadamard operators defined for the relevant qudit subspace are

$$\bar{Z} \equiv |2,0\rangle \langle 2,0| - |0,1\rangle \langle 0,1| , \tag{44a}$$

$$\bar{H} \equiv \frac{1}{\sqrt{2}} (|2,0\rangle + |0,1\rangle) \langle 2,0| + \frac{1}{\sqrt{2}} (|2,0\rangle - |0,1\rangle) \langle 0,1| . \tag{44b}$$

Since $\bar{H}$ is a unitary operator, expectation value of $\bar{X}$ reduces to photon counting in a rotated basis

$$\langle \psi | \bar{X} | \psi \rangle = \langle \psi' | \bar{Z} | \psi' \rangle = | \langle 2,0 | \psi' \rangle |^2 - | \langle 0,1 | \psi' \rangle |^2 , \tag{45}$$

where $|\psi'\rangle = \bar{H} |\psi\rangle$. The expectation values for the other Hamiltonian terms of Eq. (41) can be similarly expressed. The operator $\bar{H}$ can be implemented with a photonic setup,[S8] whereas operators like $\bar{H}$ in cQED approach can be implemented by driving cascaded three-

wave or four-wave mixing transitions using a dispersively coupled ancilla qubit, such as $|2, 0, g\rangle \leftrightarrow |0, 0, e\rangle \leftrightarrow |0, 1, g\rangle$, where $|g\rangle$ and $|e\rangle$ represent the ground and excited states of the ancilla.[S9–S11] A potentially more scalable approach for computing the expectation value of photon transfer operators between arbitrary multimode Fock states is the recently introduced subspace tomography in cQED,[S12] which does not rely on the $\bar{H}$ operators and instead uses phase space displacement operations that can be implemented efficiently.

Subspace tomography for computing photon transfer expectation values

The cQED-based subspace tomography approach described in Ref. S12 can be implemented with the help of an ancilla transmon qutrit and can be divided into two broad parts. Let us denote the three levels of the ancilla to be $|g\rangle$, $|e\rangle$, and $|f\rangle$. The first part uses a unitary operator coupled to the states $|e, g\rangle$ that transforms the full density matrix of a qumode state into a chosen subspace density matrix coupled to the $|e\rangle$ state. The second part applies phase displacement operator(s) followed by a photon-number state projection and measure the corresponding probability in the $|f\rangle$ state. We discuss the resulting expressions below.

Let us first understand the above protocol for one qumode, whose state can be represented in the Fock basis as

$$|\Psi\rangle = \sum_{n=0}^{\infty} C_n |n\rangle, \tag{46}$$

where $\{C_n\}$ are the complex-valued Fock basis coefficients. Let us assume we want to compute the expectation value of the following photon transfer operator $|j\rangle \langle k| + \text{h.c.}$

$$T_{j,k} = \langle \Psi | \big(|j\rangle \langle k| + \text{h.c.} \big) | \Psi \rangle = C_j C_k^* + C_k C_j^*, \tag{47}$$

where the operator pairing for the off-diagonal parts ensure Hermiticity. The subspace

tomography approach will choose to handle the corresponding subspace density matrix

$$\rho_{j,k} = \Big(\sum_{n=j,k} C_n \ket{n} \Big) \Big(\sum_{n=j,k} C_n^* \bra{n} \Big) = \sum_{n,m \, \in \, \mathcal{S}} C_n C_m^* \ket{n}\bra{m}, \tag{48}$$

where $\mathcal{S}$ represent the subspace chosen. Let us now apply the phase space displacement operator $D(\alpha) = e^{\alpha b^\dagger - \alpha^* b}$, which creates all possible photon excitation and deexcitation from the Fock state it acts on

$$D(\alpha) \ket{n} = \sum_{j=0}^{\infty} d_{n,j} \ket{j}, \tag{49}$$

where $\{d_{n,j}\}$ are the known and easily tunable linear coefficients associated with the displacement operator. The displacement operator transforms $\rho_{j,k}$ as

$$\begin{aligned} R_{j,k}^{(1)} &\equiv D(\alpha) \, \rho_{j,k} \, D^\dagger(\alpha) \\ &= \sum_{n,m \, \in \, \mathcal{S}} C_n C_m^* \Big[D(\alpha) \ket{n}\bra{m} D^\dagger(\alpha) \Big] \\ &= \sum_{n,m \, \in \, \mathcal{S}} C_n C_m^* \sum_{j,k \, \in \, \mathbb{N}} d_{n,j} \, (d_{m,k})^* \, \ket{j}\bra{k}. \end{aligned} \tag{50}$$

The final observable can now be represented as

$$R_{j,k,p}^{(2)} \equiv \mathrm{Tr}(\ket{p}\bra{p} R_{j,k}^{(1)} \ket{p}\bra{p}) = \sum_{n,m \, \in \, \mathcal{S}} C_n C_m^* \, d_{n,p} \, (d_{m,p})^*. \tag{51}$$

Assuming all $\{d_{n,p}\}$ coefficients to be real-valued, Eq. (51) can be rewritten as

$$\begin{aligned} R_{j,k,p}^{(2)} &= \sum_{n,m \, \in \, \mathcal{S}} d_{n,p} \, d_{m,p} \, C_n C_m^* \\ &= d_{j,p} \, d_{j,p} \, C_j C_j^* + d_{k,p} \, d_{k,p} \, C_k C_k^* + d_{j,p} \, d_{k,p} \, (C_j C_k^* + C_k C_j^*) \\ &= d_{j,p}^2 \, | \braket{j|\Psi} |^2 + d_{k,p}^2 \, | \braket{k|\Psi} |^2 + d_{j,p} \, d_{k,p} \, T_{j,k}. \end{aligned} \tag{52}$$

Since $R^{(2)}_{j,k,p}$ is the observable for the subspace tomography and $\{|\langle j|\Psi\rangle|^2\}$ can be computed by photon number counting, the expectation value for the photon transfer operator can be computed as

$$T_{j,k} = \frac{1}{d_{j,p}\, d_{k,p}} \left(R^{(2)}_{j,k,p} - d^2_{j,p}\,|\langle j|\Psi\rangle|^2 - d^2_{k,p}\,|\langle k|\Psi\rangle|^2 \right). \tag{53}$$

The generalization of the above approach to N number of qumodes is straightforward with one phase space displacement operators acting on each of the qumodes. In this case, we want to compute the expectation value of the photon transfer operator

$$T_{\mathbf{j,k}} = \langle\Psi|\big(\,|\mathbf{j}\rangle\,\langle\mathbf{k}| + \text{h.c.}\big)|\Psi\rangle, \tag{54}$$

where $\mathbf{j}$ is a vector of natural numbers and $|\mathbf{j}\rangle \equiv |j_1,\cdots,j_N\rangle_B$ is a bosonic Fock state. The corresponding subspace density matrix is

$$\rho_{\mathbf{j,k}} = \left(\sum_{\mathbf{n}=\mathbf{j,k}} C_{\mathbf{n}}\,|\mathbf{n}\rangle \right) \left(\sum_{\mathbf{n}=\mathbf{j,k}} C^*_{\mathbf{n}}\,\langle\mathbf{n}| \right) = \sum_{\mathbf{n,m}\,\in\,\mathcal{S}} C_{\mathbf{n}} C^*_{\mathbf{m}}\,|\mathbf{n}\rangle\,\langle\mathbf{m}|, \tag{55}$$

and the experimental observables are

$$R^{(1)}_{\mathbf{j,k}} \equiv D_N(\alpha)\cdots D_1(\alpha)\,\rho_{\mathbf{j,k}}\,D^\dagger_1(\alpha)\cdots D^\dagger_N(\alpha), \tag{56a}$$

$$R^{(2)}_{\mathbf{j,k,p}} \equiv \text{Tr}(|\mathbf{p}\rangle\,\langle\mathbf{p}|\,R^{(1)}_{\mathbf{j,k}}\,|\mathbf{p}\rangle\,\langle\mathbf{p}|), \tag{56b}$$

where $D_p(\alpha)$ is the displacement operator acting on the p-th qumode and $|\mathbf{p}\rangle\,\langle\mathbf{p}|$ is the multimode projection operator. Similar to discussion above, $T_{\mathbf{j,k}}$ can then be expressed as

$$T_{\mathbf{j,k}} = \frac{1}{\prod_{i=1}^{N} d_{j_i,p_i}\, d_{k_i,p_i}} \left[R^{(2)}_{\mathbf{j,k,p}} - \left(\prod_{i=1}^{N} d^2_{j_i,p_i}\right)|\langle\mathbf{j}|\Psi\rangle|^2 - \left(\prod_{i=1}^{N} d^2_{k_i,p_i}\right)|\langle\mathbf{k}|\Psi\rangle|^2 \right]. \tag{57}$$

Thus, it is possible to compute the expectation value of any photon transfer operator of the form $|\mathbf{j}\rangle\,\langle\mathbf{k}| + \text{h.c.}$ using the subspace tomography approach.

Hybrid variational approach

We have all the tools needed for applying a hybrid quantum-classical variational algorithm for finding the ground state energy of the dihydrogen molecule

$$\min_{\psi} E = \frac{\langle \psi | H_B | \psi \rangle}{\langle \psi | \psi \rangle}, \tag{58}$$

where $|\psi\rangle$ is a bosonic trial state and H_B is the mapped bosonic Hamiltonian in Eq. (41). The hybrid algorithm can assign the computation of the expectation value in Eq. (58) to a bosonic device while the energy function is optimized in a classical processor. Similar to the hybrid algorithms designed for quantum computers with qubits, one needs a robust ansatz for $|\psi\rangle$ for the minimization in Eq. (58).

We explore the universal bosonic ansatz of two qumodes for the mapped bosonic Hamiltonian of Eq. (41) here. Universal control of qumodes requires non-Gaussian resources,[S13,S14] which in cQED can be provided by the third or higher-order nonlinearity of the ancilla Josephson qubits or couplers.[S15–S20] Multiple non-Gaussian elementary gates in cQED can be used to construct a universal gate set, including, most notably, the ancilla-controlled rotation (native for dispersive Hamiltonian),[S21] the selective number-dependent arbitrary phase (SNAP) gate,[S15–S17] and the conditional displacement gate.[S18,S22] For example, one possible way to implement an arbitrary multi-qumode unitary can be achieved by a sequence of echoed conditional displacement (ECD) gates

$$ECD(\beta) = |e\rangle \langle g| \otimes D(\beta/2) + |g\rangle \langle e| \otimes D(-\beta/2), \tag{59}$$

and ancilla rotations

$$R(\theta, \varphi) = e^{-i\frac{\theta}{2}(\sigma_x \cos\varphi + \sigma_y \sin\varphi)}, \tag{60}$$

where $D(\alpha) = \exp(\alpha b^\dagger - \alpha^* b)$ is the one-qumode displacement operator, $|g\rangle, |e\rangle$ are the ground and excited states of the ancilla qubit, and σ_x, σ_y are the one-qubit Pauli operators.[S22]

Thus, a general ansatz for any bosonic Hamiltonian of two qumodes can be written as

$$|\psi\rangle = U_B(\boldsymbol{\beta}_B, \boldsymbol{\theta}_B, \boldsymbol{\varphi}_B) \cdots U_1(\boldsymbol{\beta}_1, \boldsymbol{\theta}_1, \boldsymbol{\varphi}_1) \left(|g\rangle \otimes |0,0\rangle_B \right), \tag{61}$$

where the initial state for the one ancilla qubit and the two qumodes is $|g,0,0\rangle$ and the U_j unitary is defined as

$$U_j = \left(|e\rangle \langle g| \otimes \mathbb{I} \otimes D(\beta_{2,j}/2) + |g\rangle \langle e| \otimes \mathbb{I} \otimes D(-\beta_{2,j}/2) \right) \left(R(\theta_{2,j}, \varphi_{2,j}) \otimes \mathbb{I} \otimes \mathbb{I} \right)$$
$$\times \left(|e\rangle \langle g| \otimes D(\beta_{1,j}/2) \otimes \mathbb{I} + |g\rangle \langle e| \otimes D(-\beta_{1,j}/2) \otimes \mathbb{I} \right) \left(R(\theta_{1,j}, \varphi_{1,j}) \otimes \mathbb{I} \otimes \mathbb{I} \right). \tag{62}$$

The two-qumode ansatz of Eq. (61) has B number of U_j blocks and is illustrated in Figure S3. The strategy of using an ancilla qubit rotation and ECD gates can be similarly extended for any number of qumodes.[S22] Additional strategies for multi-mode control such as based on the conditional-NOT displacement[S20] and photon blockade[S19] have also been demonstrated recently.

Specifically for the ground state of H_2 molecule in a minimal basis, the only relevant Slater determinant basis states are $|0,1\rangle_F$ and $|2,3\rangle_F$,[S23] which becomes the qumode Fock basis states $|0,0\rangle_B$ and $|0,2\rangle_B$ after the state mapping. This means the general ansatz of Eq. (61) can be applied to find the ground state of H_2 molecule, even without optimizing
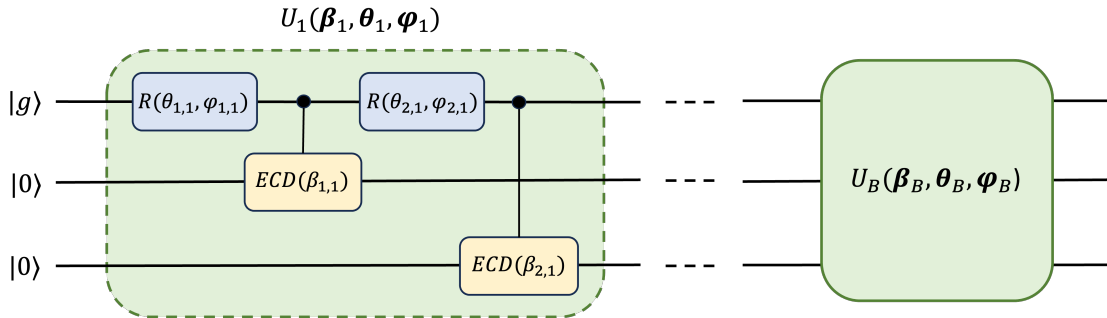

Figure S3: The universal bosonic ansatz for two qumodes with an ancilla qubit, following Ref. S22. The qubit-qumode circuit is initialized in the state $|g\rangle \otimes |0,0\rangle_B$ and then a block of ECD gates and qubit rotations are acted sequentially, as defined in Eq. (61).
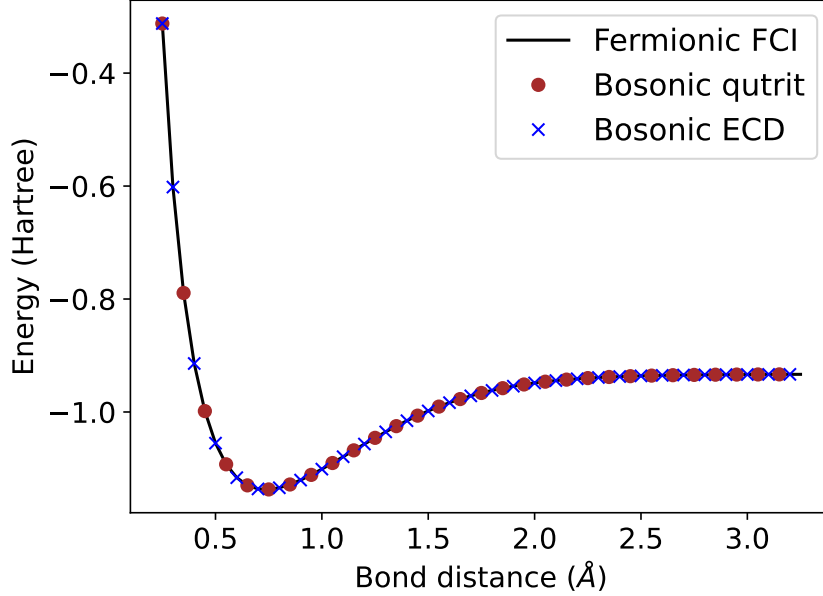
Figure S4: Ground state energies of the dihydrogen molecule in the STO-3G minimal basis for different H–H bond distances. The black line represents the exact energies in the basis of Slater determinants. The brown dots and blue crosses represent the mapped bosonic variational methods. Both the bosonic qutrit ansatz (brown dots) and the ECD-rotation ansatz (blue crosses) of Eq. (63) reproduce the exact ground state energies. For the ECD-rotation ansatz, the results are shown for $B = 2$ blocks.

the parameters on the first qumode. In that case, the following reduced version of Eq. (61) is sufficient for the ground state of H_2 molecule[S18]

$$|\psi\rangle = U_B(\beta_B, \theta_B, \varphi_B) \cdots U_1(\beta_1, \theta_1, \varphi_1) \left(|g\rangle \otimes |0,0\rangle_B \right), \tag{63a}$$

$$U_j = \left(|e\rangle \langle g| \otimes \mathbb{I} \otimes D(\beta_j/2) + |g\rangle \langle e| \otimes \mathbb{I} \otimes D(-\beta_j/2) \right) \left(R(\theta_j, \varphi_j) \otimes \mathbb{I} \otimes \mathbb{I} \right), \tag{63b}$$

where B is the number of blocks and $\{\beta_j, \theta_j, \phi_j\}$ needs to be optimized following Eq. (58). As shown in Figure S4, the ECD-rotation ansatz of Eq. (63) with only $B = 2$ blocks can reproduce the exact ground state energies for different H–H bond distances. Since the H_B defined in Eq. (41) can be thought of as a Hamiltonian of two qutrits, starting from the initial state $|0,0\rangle_B$ and applying $e^{-2i\theta\,(-i|0\rangle\langle 2|+\text{h.c.})}$, which is a qutrit R_y gate,[S24,S25] to the

second qumode is also an legitimate ansatz for the ground state, where the the scalar θ is optimized following Eq. (58). As shown in Figure S4, both the general ECD-rotation and the qutrit ansatze can reach the exact ground state energies of the H_2 molecule. It is important to note that the expectation value of H_B for any Fock basis state that is absent in H_B is naturally zero, which allows the design of flexible bosonic ansatz without contaminating the trial energy in Eq. (58), while potentially boosting the optimization.

References

(S1) Szabo, A.; Ostlund, N. S. *Modern Quantum Chemistry*; Dover Publications, 1996.

(S2) Dhar, A.; Mandal, G.; Suryanarayana, N. V. Exact operator bosonization of finite number of fermions in one space dimension. *J. High Energy Phys.* **2006**, *2006*, 118.

(S3) Ohta, K. New bosonic excitation operators in many-electron wave functions. *Int. J. Quantum Chem.* **1998**, *67*, 71.

(S4) Whitfield, J. D.; Biamonte, J.; Aspuru-Guzik, A. Simulation of electronic structure Hamiltonians using quantum computers. *Mol. Phys.* **2011**, *109*, 735.

(S5) Divochiy, A.; Marsili, F.; Bitauld, D.; Gaggero, A.; Leoni, R.; Mattioli, F.; Korneev, A.; Seleznev, V.; Kaurova, N.; Minaeva, O., et al. Superconducting nanowire photon-number-resolving detector at telecommunication wavelengths. *Nature Photon.* **2008**, *2*, 302.

(S6) Kardynał, B.; Yuan, Z.; Shields, A. An avalanche-photodiode-based photon-number-resolving detector. *Nature Photon.* **2008**, *2*, 425.

(S7) Wang, C. S.; Curtis, J. C.; Lester, B. J.; Zhang, Y.; Gao, Y. Y.; Freeze, J.; Batista, V. S.; Vaccaro, P. H.; Chuang, I. L.; Frunzio, L.; Jiang, L.; Girvin, S. M.;

Schoelkopf, R. J. Efficient Multiphoton Sampling of Molecular Vibronic Spectra on a Superconducting Bosonic Processor. *Phys. Rev. X* **2020**, *10*, 021060.

(S8) Xu, L.; Zhou, M.; Tao, R.; Zhong, Z.; Wang, B.; Cao, Z.; Xia, H.; Wang, Q.; Zhan, H.; Zhang, A.; Yu, S.; Xu, N.; Dong, Y.; Ren, C.; Zhang, L. Resource-Efficient Direct Characterization of General Density Matrix. *Phys. Rev. Lett.* **2024**, *132*, 030201.

(S9) Hofheinz, M.; Weig, E.; Ansmann, M.; Bialczak, R. C.; Lucero, E.; Neeley, M.; O'connell, A.; Wang, H.; Martinis, J. M.; Cleland, A. Generation of Fock states in a superconducting quantum circuit. *Nature* **2008**, *454*, 310.

(S10) Gao, Y. Y.; Lester, B. J.; Zhang, Y.; Wang, C.; Rosenblum, S.; Frunzio, L.; Jiang, L.; Girvin, S. M.; Schoelkopf, R. J. Programmable Interference between Two Microwave Quantum Memories. *Phys. Rev. X* **2018**, *8*, 021073.

(S11) Zhang, Y.; Lester, B. J.; Gao, Y. Y.; Jiang, L.; Schoelkopf, R. J.; Girvin, S. M. Engineering bilinear mode coupling in circuit QED: Theory and experiment. *Phys. Rev. A* **2019**, *99*, 012314.

(S12) Gertler, J. M.; van Geldern, S.; Shirol, S.; Jiang, L.; Wang, C. Experimental Realization and Characterization of Stabilized Pair-Coherent States. *PRX Quantum* **2023**, *4*, 020319.

(S13) Lloyd, S.; Braunstein, S. L. Quantum Computation over Continuous Variables. *Phys. Rev. Lett.* **1999**, *82*, 1784.

(S14) Braunstein, S. L.; van Loock, P. Quantum information with continuous variables. *Rev. Mod. Phys.* **2005**, *77*, 513.

(S15) Krastanov, S.; Albert, V. V.; Shen, C.; Zou, C.-L.; Heeres, R. W.; Vlastakis, B.; Schoelkopf, R. J.; Jiang, L. Universal control of an oscillator with dispersive coupling to a qubit. *Phys. Rev. A* **2015**, *92*, 040303.

(S16) Heeres, R. W.; Vlastakis, B.; Holland, E.; Krastanov, S.; Albert, V. V.; Frunzio, L.; Jiang, L.; Schoelkopf, R. J. Cavity State Manipulation Using Photon-Number Selective Phase Gates. *Phys. Rev. Lett.* **2015**, *115*, 137002.

(S17) Fösel, T.; Krastanov, S.; Marquardt, F.; Jiang, L. Efficient cavity control with SNAP gates. *arXiv preprint arXiv:2004.14256* **2020**,

(S18) Eickbusch, A.; Sivak, V.; Ding, A. Z.; Elder, S. S.; Jha, S. R.; Venkatraman, J.; Royer, B.; Girvin, S. M.; Schoelkopf, R. J.; Devoret, M. H. Fast universal control of an oscillator with weak dispersive coupling to a qubit. *Nat. Phys.* **2022**, *18*, 1464.

(S19) Chakram, S.; He, K.; Dixit, A. V.; Oriani, A. E.; Naik, R. K.; Leung, N.; Kwon, H.; Ma, W.-L.; Jiang, L.; Schuster, D. I. Multimode photon blockade. *Nat. Phys.* **2022**, *18*, 879.

(S20) Diringer, A. A.; Blumenthal, E.; Grinberg, A.; Jiang, L.; Hacohen-Gourgy, S. Conditional-not Displacement: Fast Multioscillator Control with a Single Qubit. *Phys. Rev. X* **2024**, *14*, 011055.

(S21) Vlastakis, B.; Kirchmair, G.; Leghtas, Z.; Nigg, S. E.; Frunzio, L.; Girvin, S. M.; Mirrahimi, M.; Devoret, M. H.; Schoelkopf, R. J. Deterministically encoding quantum information using 100-photon Schrödinger cat states. *Science* **2013**, *342*, 607.

(S22) You, X.; Lu, Y.; Kim, T.; Kurkcuoglu, D. M.; Zhu, S.; van Zanten, D.; Roy, T.; Lu, Y.; Chakram, S.; Grassellino, A.; Romanenko, A.; Koch, J.; Zorzetti, S. Crosstalk-Robust Quantum Control in Multimode Bosonic Systems. *Phys. Rev. Appl.* **2024**, *22*, 044072.

(S23) Lanyon, B. P.; Whitfield, J. D.; Gillett, G. G.; Goggin, M. E.; Almeida, M. P.; Kassal, I.; Biamonte, J. D.; Mohseni, M.; Powell, B. J.; Barbieri, M., et al. Towards quantum chemistry on a quantum computer. *Nature Chem.* **2010**, *2*, 106.

(S24) Arrazola, J. M.; Jahangiri, S.; Delgado, A.; Ceroni, J.; Izaac, J.; Száva, A.; Azad, U.; Lang, R. A.; Niu, Z.; Di Matteo, O., et al. Differentiable quantum computational chemistry with PennyLane. *arXiv preprint arXiv:2111.09967* **2021**,

(S25) Goss, N.; Morvan, A.; Marinelli, B.; Mitchell, B. K.; Nguyen, L. B.; Naik, R. K.; Chen, L.; Jünger, C.; Kreikebaum, J. M.; Santiago, D. I.; Wallman, J. J.; Siddiqi, I. High-fidelity qutrit entangling gates for superconducting circuits. *Nat. Commun.* **2022**, *13*, 7481.